Recibido el 29-08-17
Aprobado el 19-02-18

SYNTHESIS OF Ni-Cu CATALYSTS BY IMPREGNATION TO OBTAIN CARBON NANOFIBERS BY CATALYTIC DECOMPOSITION OF METHANE

Jonathan Almirón Baca[a*], Hermann Alcázar Rojas[a], Rossibel Churata Añasco[a], María Vargas Vilca[a], Leopoldo Alcázar Rojas[b], Fabiana Fim[c]

ABSTRACT

This paper reports the synthesis by impregnation method and the characterization of Ni-Cu catalyst supported on alumina (Al_2O_3). Three catalysts with different Ni-Cu atomic ratios (7:1, 9:1 and 11:1) were synthesized. These catalysts were characterized by X-ray diffraction (XRD), X-ray fluorescence (XRF), scanning electron microscopy (SEM), thermogravimetric analysis (TGA), textural BET analysis and TPR. In addition, it has been produced carbon nanofibers by catalytic decomposition of methane at 600 °C. The results suggest that nickel loading influences the carbon deposited on. Thus, the catalyst with greater Ni:Cu atomic ratio of 11:1 showed the better carbon yield (19,4 gC/gcat). Moreover, the structural properties of the carbon deposited are dependent of the catalyst composition, going on from a thin and long carbon over Ni-Cu 11:1 catalyst to a broad and shorter carbon over Ni:Cu 7:1 and 9:1 catalysts.

Key words: Supported catalyst, Ni-Cu/Al_2O_3, impregnation, decomposition of methane, carbon nanofiber.

SINTESIS DE CATALIZADORES EN BASE A Ni-Cu POR IMPREGNACIÓN PARA LA OBTENCIÓN DE NANOFIBRAS DE CARBONO POR DEPOSICIÓN CATALÍTICA DEL METANO

RESUMEN

Se prepararon y caracterizaron catalizadores de Níquel–Cobre soportados sobre alúmina (Al_2O_3) mediante el método de impregnación, en el cual se realizaron variaciones en las proporciones Ni:Cu de 7:1, 9:1 y 11:1. Se caracterizó el catalizador por difracción de rayos X, Fluorescencia de Rayos X, microscopia electrónica de barrido, análisis Terrmogravimétrico y la medición de superficie de área BET; además se realizaron ensayos de síntesis de nanofibras

[a] Escuela Profesional de Ingeniería Mecánica, Mecánica Eléctrica y Mecatrónica, Facultad de Ciencias e Ingenierías Físicas y Formales, Universidad Católica de Santa María UCSM, Samuel Velarde N° 320, Arequipa, Perú, *jalmiron@ucsm.edu.pe
[b] Departamento de Engenharia Química, Universidade Federal da Paraíba UFPB, João Pessoa, Brasil.
[c] Departamento de Engenharia Materiais , Universidade Federal da Paraíba UFPB, João Pessoa, Brasil.

de carbono mediante la descomposición catalítica de metano a 600°C. Los resultados sugieren que la carga del Níquel influye en la deposición de carbono, siendo la relación con el mayor contenido de Níquel (Ni:Cu 11:1) la que mostró mayor rendimiento (19,4 gC/gcat). Además las propiedades estructurales del carbono depositado dependían de la composición del catalizador, pasando de un carbono fino y largo sobre el catalizador Ni:Cu 11:1 a un carbono ancho y algo más corto sobre las muestra de Ni:Cu 7:1 y 9:1.

Palabras clave: Catalizador soportado, Ni-Cu/Al_2O_3, impregnación, descomposición de metano, nanofibra de carbono.

INTRODUCTION

In recent years, the catalytic decomposition of methane (CDM) has attracted the attention of the scientific community due to its potential to produce CO_x-free hydrogen[1] and carbon deposited on the catalyst in the shape of layers, filaments, fibers, or nanotubes[2]. A broad range of potential applications, for this carbon, can be identified as: catalysts, catalyst supports, composite materials, among others[3].

Catalyst based on Ni, Fe and Co metals over metal oxide supports (Al_2O_3 or SiO_2) are widely used for the growth of carbon nanofibers (CNFs) from methane[4]. Especially nickel catalyst with high loading is commonly used for the catalytic decomposition of methane (CDM) into hydrogen and carbon[4]. Among methane decomposition reactions, Ni based catalyst has shown a better performance than Fe and Co, in a reaction range temperature between 500 °C and 700 °C[5].

Temperatures higher than 600 °C proved to be very active for Ni/Al_2O_3, followed by Co/Al_2O_3 and Fe/Al_2O_3[6]. But, higher temperatures can destabilize the catalyst and a promotor, such as copper, must be added to ensure stability and durability, avoiding its deactivation[7]. It was reported that the use copper as promoter increases the methane decomposition activity of nickel, improves nickel dispersion over the support, and enhances thermal stability of the catalyst[7].

An issue in catalyst preparation procedure is to seek for a method that allows exposing the maximum active sites to the reagents. In a metallic supported catalyst, the goal is to disperse as much as possible the metallic active phase (Ni) over the support (Al_2O_3), in order to maximize the surface density of the active sites and the catalyst performance[5]. The literature reports several preparation methods to achieve this desire metal dispersion. Precipitation, co-precipitation and wet-impregnation are the preparation methods most frequently mentioned. The last one, wet-impregnation, has a simple procedure and gives a better way of controlling metal dispersion by the manipulation of experimental process variables, for this reason it has been chosen for the preparation of the catalysts in this work.

Previous works, with NiAl and NiCuAl catalysts, showed the influence of the preparation methods to the observed yields for hydrogen and carbon fibers in the catalytic decomposition of methane[8]. They concluded that the preparation method and addition of copper to the Ni-supported catalyst had a major influence on the nickel dispersion and the mean size of the nickel crystallites[9]. The domain sizes of NiO in the calcined samples are highly dependent on the preparation method of the catalyst used. Therefore, fusion method seems to enhance the formation of NiO with smaller crystal sizes; while on the other hand, the impregnation method promotes the formation of higher NiO crystallites. These domain sizes are in contrast with the results obtained using Al as a textural promoter, in which case impregnation and fusion methods led to obtain similar NiO domain sizes while the co-precipitation method promotes the formation of very small NiO crystallites[8].

This paper reports the synthesis of Ni-Cu catalysts supported over alumina with Ni/Cu atomic ratios of 7:1, 9:1 and 11:1 prepared by thermal decomposition in the first step and then supported over alumina by successive copper-nickel impregnation-calcination, characterized by X-ray diffraction (XRD), X-ray fluorescence (XRF), scanning electron microscopy (SEM), thermogravimetric analysis (TGA) and nitrogen sorption (BET analysis). Catalytic tests for the decomposition of methane were performed in a customized unit (as detailed in the experimental section) at 600°C.

EXPERIMENTAL DETAILS

Catalyst preparation

Three Ni-Cu based catalysts supported over alumina (Al_2O_3) were prepared by thermal decomposition in the first step and then supported over alumina though impregnation with Ni:Cu atomic ratios of 7:1, 9:1, and 11:1. For notation purposes these materials are denoted as 7Ni, 9Ni and 11Ni, respectively. The support γ-Al_2O_3 was obtained from $Al(NO_3)_3.3H_2O$ P.A. precursor followed by calcination at 450 °C for 4 h.

Two stock solutions of Cu and Ni were prepared by dissolving Cu $(NO_3)_3.3H_2O$ P.A. and Ni $(NO_3)_2.6H_2O$ P.A. salts, respectively, and then diluted in distilled water. In order to have a better control of the Cu and Ni depositions, the impregnations were done sequentially[10]. The impregnation was done first with Cu and then by Ni successively, employing similar procedures. In a recipient, loaded previously with alumina, is added the Cu stock solution and kept stirred (450 rpm) at 70 °C for 3 h. The impregnated alumina is dried at 105°C for 3h or until constant weight is attained, milled, and calcined at 350°C for 3 h. After cooling, the impregnation procedure is repeated for Ni stock solution. The resultant suspension is aged for 24 h at room temperature, dried for 6 h at 105°C, milled and calcined at 450°C in a muffle for 4 h8. The following reactions belong to the synthesis of catalyst:

$$4Al(NO_3)_3.3H_2O_{(s)} \xrightarrow{450\,^{\circ}C\ 4h} 2Al_2O_{3(s)} + 12NO_{2(g)} + 3O_{2(g)} + 3H_2O_{(g)} \quad (1)$$

$$2Cu(NO_3)_2.3H_2O_{(s)} \xrightarrow{350\,^{\circ}C\ 3h} 2CuO_{(s)} + 4NO_{2(g)} + O_{2(g)} + 3H_2O_{(g)} \quad (2)$$

$$2Ni(NO_3)_2.6H_2O_{(s)} \xrightarrow{450\,^{\circ}C\ 4h} 2NiO_{(s)} + 4NO_{2(g)} + O_{2(g)} + 6H_2O_{(g)} \quad (3)$$

The nominal metallic loadings are presented in Table 1.

Catalysts characterization

The X-ray fluorescence (XRF) was carried out in an EDX-720 Shimadzu spectrometer to determine the chemical composition of catalysts (in oxide base).

The structural phases of the crystalline alumina as well as the metal oxides were obtained by XRD (X Ray Diffractometry) using a Bruker (D8 Avance Davinci) diffractometer with CuKα (λ = 0,1542 nm) radiation operated at 40 kV, 40 mA with a 2θ range from 5° to 90° and a 0,6°/min scan rate.

The homogeneity and dispersion of nickel and copper oxides over the support, as well as the surface morphology, were carried out on a LEO (1430 ZEISS model) scanning electron microscope (SEM) operated at 15 kV. Every sample was pretreated previous to the scan by fixing it on a carbon tape and coated with gold by conventional sputtering techniques.

Textural analysis for the support and non-reduced catalysts samples were performed by BET adsorption and desorption isotherms of nitrogen at 77 K in an ASAP 2020 Micromeritics apparatus. The specific surface area was determined by BET analysis, while pore volume distribution and average pore diameter (D_p) were calculated by the BJH method based on the desorption isotherms of nitrogen.

Thermal behavior of the catalysts was evaluated by thermogravimetric analysis (TGA) in a TA Instruments SDT – Q60 device. The samples (10-20 mg) were loaded into aluminum crucibles and heated from 30 to 800 °C, under a linear temperature rate of 10 °C/min, for N_2 and air atmospheres with flow rates of 50 ml/min.

The metal-support and metal-metal interactions were observed through TPR tests in a Micromeritics apparatus. Before the reduction, 100 mg samples were charged into the quartz reactor and cleaned under N_2 flow at 300 °C. After cooling TPR experiments ran at 5°C/min heating rate from 25 to 800°C, with a 10% H_2 /N_2 reducing mixture flow of 25 sccm. The system was equipped with a TCD detector for monitoring the hydrogen consumption. The quantification of H2 consumption was performed using Ag_2O as standard reference.

Catalytic evaluation

The evaluation of the catalytic activity was carried out in a tubular quartz chamber, 1200 mm length and 50 mm internal diameter. The catalysts samples (approximately 200 mg) were placed on a rectangular (50 x 20 mm) alumina crucible and centered in the tubular chamber. All runs were performed at nearly atmospheric pressure.

The catalysts were activated by passing through a H_2:N_2 gas mixture (40:60) at 250 sccm for 2 h and 500 °C. Then, a N_2 stream is switched and set to 150 sccm. The temperature was arise at 20°C/min and fixed at 600 °C. Following, a CH_4-N_2 stream was aligned with 55 and 83 sccm flow rates respectively, taking this event as the initial point for the methane decomposition

reaction. The reaction was carried for 5 hours and then cooled to room temperature. The solid products deposited were weighed and characterized by SEM.

Microactivity Test

The microactivity test was done in a 1200C LTG-01 reactor, CI-Precision thermobalance provided with massflow controllers. A 10 mg of sample is charged in a Pt mesh. The sample was cleaned in N_2 flow (200 sccm) from room to 500 °C. Then H_2 is feed in a 12% H_2/N_2 flow (200 SCCM) until the reduction is over. Again the system is cleaned with N_2 and a then heated to reaction temperature. A 60% CH_4/N_2 reaction mixture is switched to begin the reaction. The reaction is run over time until stabilization (no mass change) is detected.

RESULTS AND DISCUSSION

Catalysts characterization

Table 1 presents the compositions (from the EDX) and textural parameters of the different Ni-Cu calcined materials. Taking the pure alumina (Al) as texture reference, the other three materials exhibit the following common departure pattern: An increase in the nickel loading results in a decrease in specific area and an increment in the pore diameter, as reported by Ashour[9]. This is typical of micro-pore blockage, due to the deposition of the Ni and Cu oxides. When comparing 7Ni with our reference (Al) it seems to follow the stated pattern, but the pore volume and specific area of 7Ni is greater than Al, telling that new pores (mesopores) are created.

Table 1. Chemical characteristics and textural properties of the catalysts and the support.

Sample	% NiO	% CuO	% Al_2O_3	BET specific area (S_{BET}) (m^2/g)	Pore Volume (V_P) (cm^3/g)	Pore Diameter (D_P) (Å)
Ni:Cu 7:1	20,23	3,65	76,13	181,48	0,2218	47,203
Ni:Cu 9:1	28,38	3,84	67,78	169,52	0,1888	49,669
Ni:Cu 11:1	37,43	4,05	58,52	155,24	0,2065	51,392
Alumina	-	-	100,00	175,53	0,1832	41,322

For the other modified materials, the specific areas are below the reference, as expected, but again the 9Ni catalyst presents a higher pore volume[7]. This behavior can be explained, considering the alumina not only as a support, but as a texture promoter to prevent the coalescence of metallic particles[5]. Probably, the metallic (or oxide) particles finely disperse can present an extra area and pore volume simultaneously with a pore blockage of the support. These are two contrary effects and apparently, at low loadings (Ni:Cu 7), the first effect prevails and the second effect is more intense for high loadings (Ni:Cu 11, Ni:Cu 9).

As shown in Figure 1, according to IUPAC classification, the isotherms of all the catalysts belong to type IV[11]. They exhibit the hysteresis cycle and are characterized for being mesoporous solids.

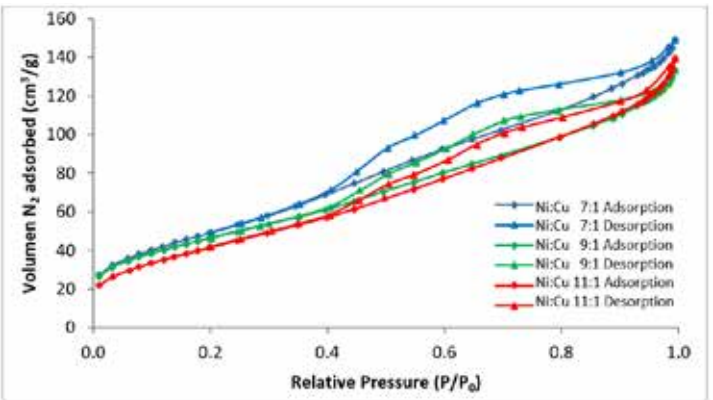

Figure 1. Adsorption–desorption isotherms of catalysts: Catalysts impregnated with nitrate salts.

The XRD profiles of the support and synthetized catalysts are depicted in Figure 2. The XRD spectra of the Ni-Cu catalysts, despite the intensity of the Ni peaks, did not show any significant difference. As expected, more Ni loading results in higher Ni peaks. It was observed at 68° a wide peak of low intensity attributed to the support, in concordance with Orellana *et al.*[12] and De Llobet *et al.*[13], that assigned it to gamma alumina. Similarly, Yalamac *et al.*[14] reported that the XRD spectrum of alumina presents a well-defined and with high intensity peak corresponding to alpha phase (α-Al_2O_3), while those of the gamma phase (γ-Al_2O_3) were barely noticeable with a peak at 46°, indicating that γ-Al_2O_3 exhibits a low intensity signal compared to α-Al_2O_3. This peak has been obtained in our sample of the support that is shown in Figure 2, as well. Therefore, the XRD support spectra in the present research indicates the presence of γ-Al2O3 which is amorphous.

The peaks at 37,2°, 43,2°, 62,8° and 75,3° in the XRD have been assigned to NiO by Jiménez[15] and De Llobet *et al.*[16], in accordance with the letter (JCPDS 78-0645) for a mixture of nickel and copper oxide. Lee *et al.*[17] attribute the 43,3° and 62,8° peaks to the crystalline structure of (Ni-Cu)O. Besides it was observed a few formations of spinel like-structures ($NiAl_2O_4$) with characteristics peaks in angular positions at 2θ 37.0°, 45.5°, 59.5° and 66.2° (Li J., y otros, 2016). This structure with strong interaction metal - support reduces the deposition of carbon.

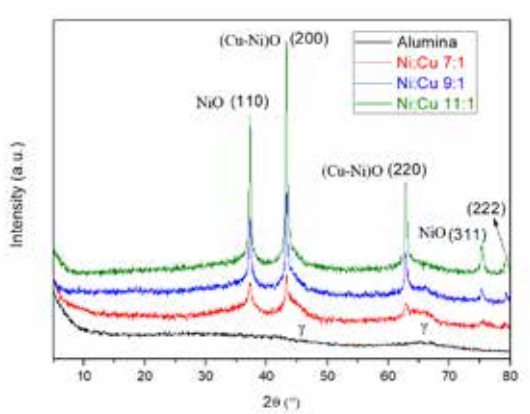

Figure 2. Diffractograms of the support and Ni-Cu/Al_2O_3 catalysts.

The morphological appearance of the 7Ni, 9Ni and 11Ni oxide catalysts is shown in Figure 3(a), 3(b) and 3(c) respectively. The samples appear as large agglomerates of particles. The sizes of individual particles in the agglomerate cannot be clearly set. The small particles of Ni and Cu supported on Al_2O_3 structures are similar to those observed in previous works[7,16]. Also, it was identified the formation of these agglomerates, that were hardly obtained by SEM, TEM analysis would preferable.

Figure 3 (d) shows the micrograph of alumina support, which evidences an irregular size and shape as it was expected according to the alumina diffractogram (amorphous phase). It is important to mention that Orellana *et al.*[12] carried out a SEM analysis to ɤ-Al_2O_3, the micrograph neither had a homogeneous shape or size; however, is observed an agglomerate of the nanoparticles. In addition, Yalamac *et al.*[14] had observed that the shape of the gamma alumina are mainly vermicular (worm type) or small corrugated platelets.

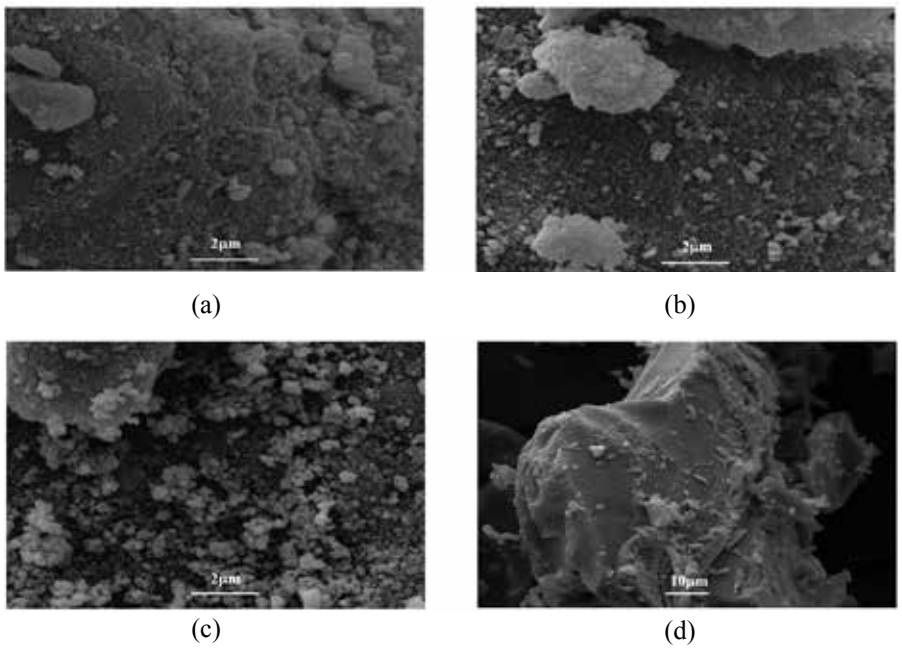

Figure 3. SEM micrographs of Ni-Cu/Al2O3 fresh catalysts and support: (a) Ni:Cu 7:1 catalyst; (b) Ni:Cu 9:1 catalyst; (c) Ni:Cu 11:1 catalyst and (d) support.

The thermal stability of the calcined catalysts was studied by TG-DTG profiles, depicted in Figure 4, in an oxidant and inert flow using nitrogen and air respectively.

The results for all catalysts in both atmospheres are similar, in other words, the weight loss occurs at temperatures between 80-200 °C that may be due to the presence of adsorbed water. At higher temperatures, no weight loss peaks were observed for the three catalysts. This behavior is expected since these are calcined materials and all thermal decompositions should already have been occurred. Nevertheless, the weight loss is greater for the material with lower Ni content (7Ni). Since adsorption is a surface process, it is in accordance with the textural results where this material presents the highest specific area. This trend is followed by the other two materials. Note that in an inert atmosphere the loss weight for every material was higher when compared with air atmosphere. This can be attributed to local equilibrium between adsorbed water and moisture content in the air.

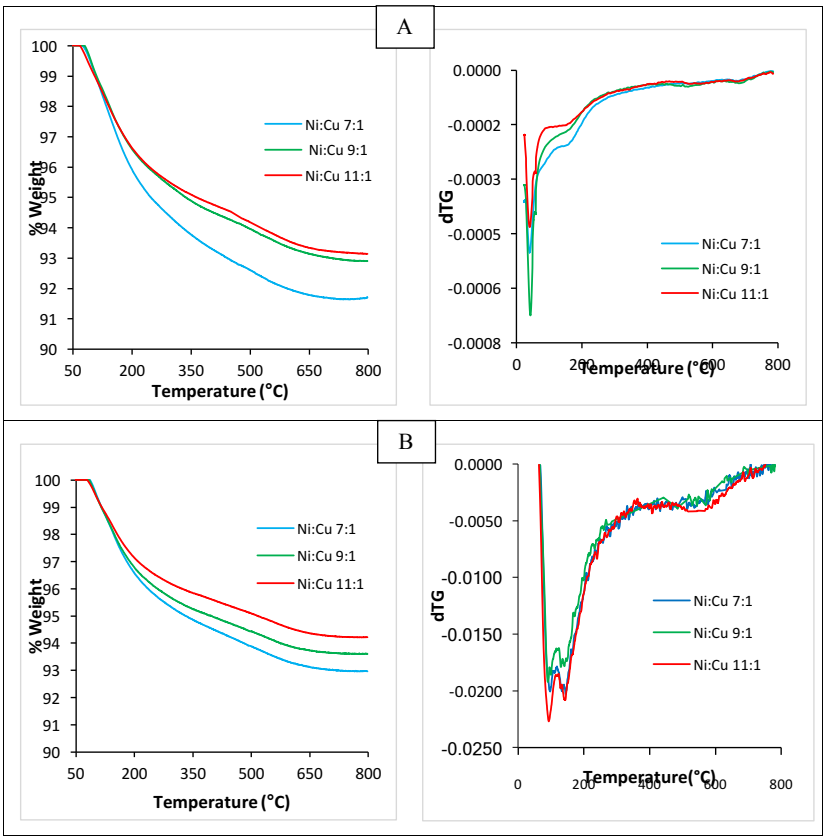

Figure 4. TGA profiles of the used catalysts in nitrogen (A) and air atmosphere (B).

Figure 5 shows the Temperature Programed Reduction (TPR) profiles of the three catalysts, identifying three zones. The hydrogen consumption increases in accordance with the metal loading (Table 2). As reported[17], the peaks around 240, 300 and 570°C correspond to Cu-Ni alloy oxide, NiO (nickel oxide isolated) and $NiOAl_2O_4$, respectively. These distribution are shown in the deconvolution of the TPR curves in Table 3 and Figure 6 for the Ni:Cu 11:1 material. The broad peak of $NiAl_2O_4$ appears as a consequence of increasing temperature (>500 ºC) due to the fact that solid state reactions are carried out between the support and the deposited phase, this occurs in all samples, almost irrespective of Ni loading. This specie appears in materials with calcination temperatures below 800°C. The first peak represents the Cu-Ni interaction and seems to follow the Ni and Cu loading. The NiO peak appears sharply at high Ni loading (Ni:Cu 11:1) and much broadly in low Ni content. A shift toward lower reduction temperature of NiO can be identify, due to the presence of Cu. Another important feature is that this phase exhibits the highest sensitivity toward the Ni loading, changing the phase percent from 27% - 34% - 49% approximately.

The following reaction shows the NiO, CuO, and $NiAl_2O_4$ hydrogenation reactions:

$$NiO. + H_2 \xrightarrow{<500\ ^\circ C} Ni + H_2O \quad (4)$$

$$CuO\text{-}NiO + H_2 \xrightarrow{<500\ ^\circ C} Cu\text{-}Ni + H_2O \quad (5)$$

$$NiAl_2O_4 + H_2 \xrightarrow{>500\ ^\circ C} Ni + Al_2O_3 + H_2O \quad (6)$$

Table 2. Reducing properties of Ni:Cu 7:1, 9:1 and 11:1 catalysts

Sample	Masa de muestra (mg)	Volumen de H2-exp. (mL-STP/g_{cat})	Volumen de H2-Teo. (mL-STP/g_{cat})
Ni:Cu 7:1	102.8	48.1	71.0
Ni:Cu 9:1	105.2	57.0	96.0
Ni:Cu 11:1	117.7	83.0	123.7

Table 3. Peak deconvolution data of TPR curves.

	Ni:Cu 11:1				Ni:Cu 9:1				Ni:Cu 7:1			
	Peak	Deviation	Area	Phase %	Peak	Deviation	Area	Phase %	Peak	Deviation	Area	Phase %
CuO-NiO	230	18.48	3.65	18.6	233.2	15.58	2.10	17.8	236.3	13.29	0.70	7.7
NiO	300	47.27	9.57	48.8	293.1	47.64	3.97	33.8	303.7	52.28	2.48	27.2
NiO-Al2O3	580	94.57	6.37	32.5	573.0	92.29	5.69	48.4	569.1	96.27	5.94	65.1

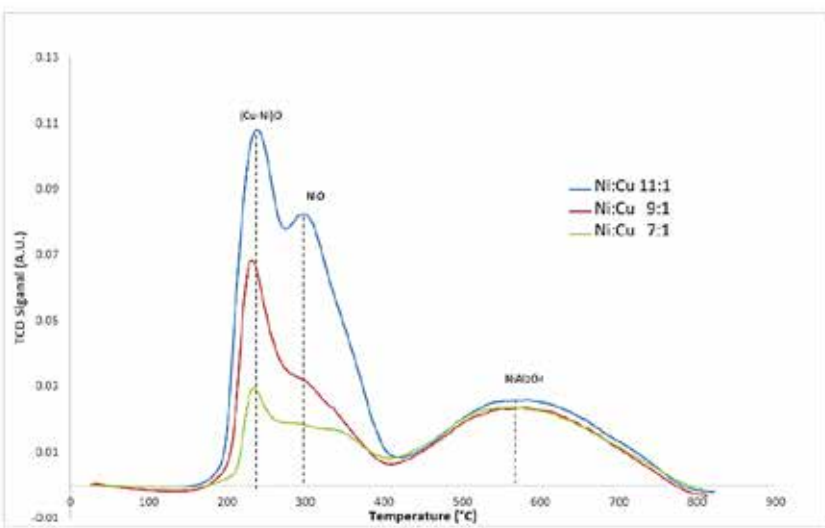

Figure 5. TPR profiles of the calcined catalysts.

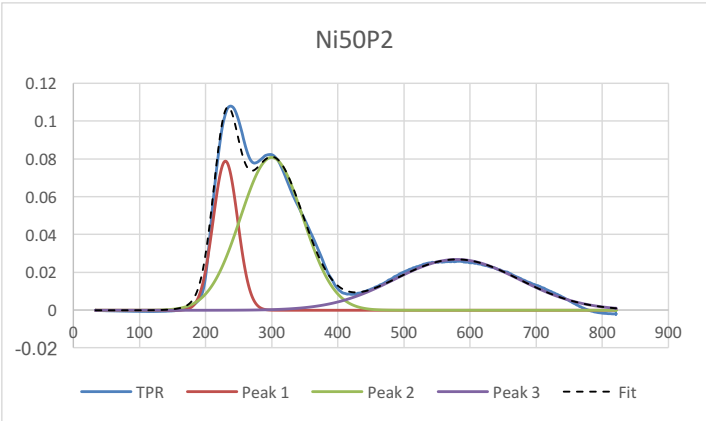

Figure 6. Deconvolution of TPR curve for NiOP2 material.

Catalytic evaluation

The results of the catalytic evaluation are depicted in Table 4. All the catalysts were tested under similar reactions conditions, taking the carbon deposited on the material as a performance and its dependence to nickel loading. As a general trend, the catalyst performance increases with the Ni loading[18]. But, when analyzing the carbon deposited per Ni loading the apparent trend is not followed, the 9Ni material appears to be the most active per Ni loading. Figure 7 shows the carbon deposited over time for 11Ni catalyst, where 82% of carbon is deposited in the first 5 hours.

Table 4. Catalytic performance at 600 °C and 5 hours of reaction

Sample	C (g)	C_g (g/g)	C_{Ni}
Ni:Cu 7:1	1,8989	9,5	46,96
Ni:Cu 9:1	3,5215	17,6	62,02
Ni:Cu 11:1	3,8826	19,4	51,83

C: carbon deposited on catalyst
C_g: carbon deposited on catalyst per catalyst weight
C_{Ni}: carbon deposited on catalyst per Ni loading

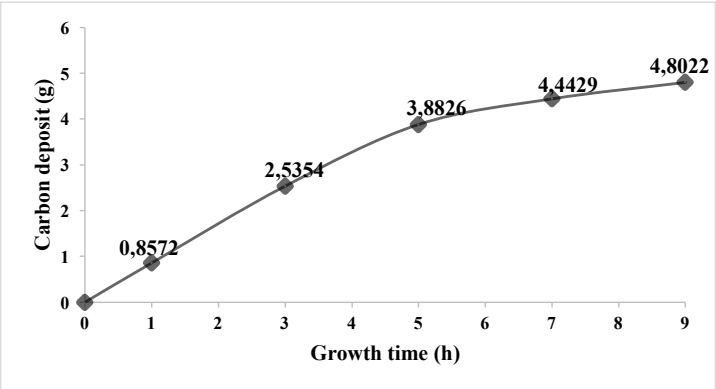

Figure 7. Carbon deposition as a function of reaction time over Ni:Cu 11:1 catalyst at 600°C.

Microactivity Test

The catalytic activity of the catalyst toward carbon formation was also studied in a differential reactor in order to have a preliminary idea of the kinetics involved is presented in Figure 8. We will focus to the initial time reaction, since at the beginning of the reaction, the surface is clean, we can attribute the slope of the curve as the intrinsic reaction rate. Surprisingly, the slope decreases with the Ni loading for the same temperature (at 600 ºC), meaning that the Ni loading itself cannot explain the reaction mechanism. As the TPR shows, there are three types of Ni species before the reduction. The $NiAl_2O_4$ seems that does not depend on Ni loading, and the nickel oxide isolated appears at high Ni loading. So the interaction Cu-Ni seems to diminish with Ni loading. This trend can explain the slope change in Figure 6 and three important conclusions can be extracted. The first is that NiAl2O4 seems that does not have the major influence in the reaction rate. Second that the interaction Cu-Ni is very important to describe the reaction rate. Third the Ni isolated has an important contribution to the reaction but not as much as the Cu-Ni alloy.

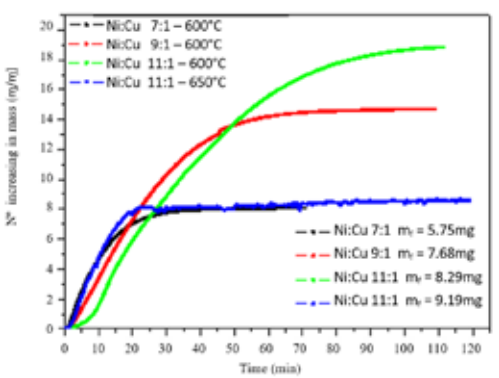

Figure 8. Kinetic of carbon deposition

SEM analysis was carried out to observe the morphology of carbon deposits obtained at 5 hours of reaction for all catalysts. Figure 9 shows the micrographs that evidence the production of carbon nanofibers (CNF) by all catalysts. The CNF obtained showed a wide range of diameters ranging from 20 to 110 nm and fibers in shape of twisted filamentous.

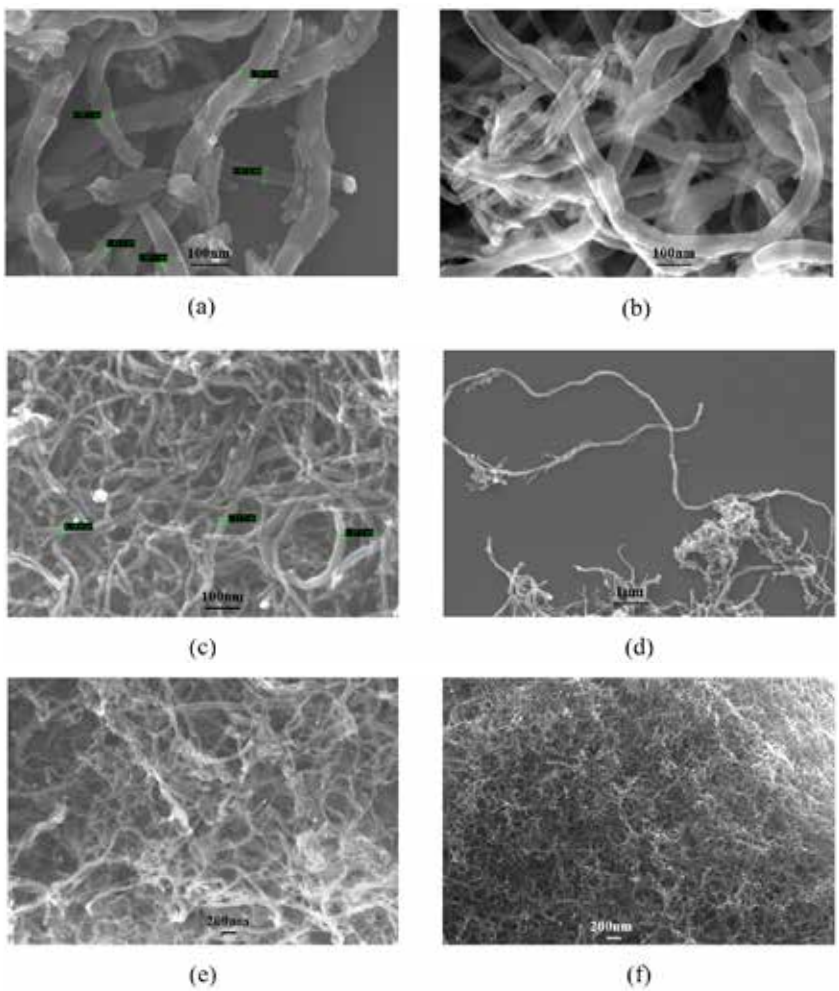

Figure 9. SEM micrographs of the products obtained by methane decomposition using Ni-Cu/Al2O3 catalysts: (a) Micrograph to 100Kx of Ni:Cu 7:1 catalyst; (b) Micrograph to 100Kx of Ni:Cu 9:1 catalyst; (c) Micrograph to 100Kx of Ni:Cu 11:1 catalyst; (d) Micrograph to 10Kx of Ni:Cu 7:1 catalyst; (e) Micrograph to 20Kx of Ni:Cu 9:1 catalyst and (f) Micrograph to 20Kx of Ni:Cu 11:1 catalyst.

It has been observed differences related to the catalyst composition, in figure 9 (a) and 9 (b), that correspond to 7Ni and 9Ni, respectively. The carbon nanofibers appear to be shorter and with larger diameters, which is consistent with the low carbon yield, than the obtained with 11Ni catalyst where the fibers are thinner and longer. What seems interest is that Ni isolated is only seen in this material, though it can be attributed to this specie the formation of this type of carbon fiber.

A quantitative analysis of the carbon fiber yields should be done in future works. A relation between carbon fiber parameters as fiber length or fiber diameters and metal loading (Cu, Ni) is not straight forward. To have a more clear view of the system a mechanism for the fiber growth must be elucidated establishing the type of site(s) that promotes this growth.

CONCLUSIONS

Three Ni-Cu catalysts supported on alumina in gamma phase (γ-Al_2O_3), synthesized by impregnation were active toward the production of carbon fibers.

The XRD results identified three species before the reduction corresponding to (Cu-Ni)O and NiO with characteristics peaks at 37,2 °, 43,2°, 62,8 °, 75,3 ° and 79,0 °. In addition, it was observed peaks at 68 ° and 46 ° (2θ) that correspond to the gamma phase (γ-Al_2O_3) of the amorphous alumina support.

The TPR showed that NiAl2O4 appears at higher temperatures from 500 ºC and does not depend directly on the Ni loadings. Besides, Cu-Ni interacts in every Ni content, but cannot explain the catalyst activity.

The catalyst composition substantially affects the methane decomposition so a higher amount of nickel (11Ni) produces a major carbon deposited (3.8826 g) than 7Ni and 9Ni catalysts with values of 1,8989 g and 3,5215 g, respectively.

The 11Ni catalyst has produced thin and elongated carbon nanofibers probably due to its nickel loading that is higher than the others catalysts; and according TPR it had the major consumption of hydrogen and therefore, major amount of active metal.

ACKNOWLEDGEMENT

The authors are grateful to CONCYTEC-FONDECYT (Proyecto PIBAP N°000141-2015) for financing this research, to the Universidad Católica de Santa María (UCSM) for co-financing and overall support, and to the Universidade Federal da Paraíba (UFPB) for their help and technical support.

REFERENCES

1. Li, Y., Li, D., & Wang, G. (2011, March). Methane decomposition to COx-free hydrogen and nano-carbon material on group 8–10 base metal catalysts: A review. *Catal. Today*, *162*(1), 1-48.
2. J., Rupprechter, G. (2015). Surface modification processes during methane decomposition on Cu-promoted Ni–ZrO2 catalysts. *Catal. Sci. Technol.*, *5*(2), 967-978.
3. Tessonnier, J.- P., & Su, D. S. (2011). Recent Progress on the Growth Mechanism of Carbon Nanotubes: A Review. *ChemSusChem*, *4*(7), 824-847.
4. Ermakova, M. A., Ermakov, D. Y., Kuvshinov, G. G., & Plyasova, L. (1999). New Nickel Catalysts for the Formation of Filamentous Carbon in the Reaction of Methane Decomposition. *J. Catal., 187*, 77-84.
5. Wang, Y., Peng, J., Zhou, C., Lim, Z.-Y., Wu, C., Ye, S., & Wang, W. G. (2014). Effect of Pr addition on the properties of Ni/Al2O3 catalysts with an application in the autothermal reforming of methane. *Int. J. Hydrogen Energy, 39*, 778-787.
6. Ogihara, H., Takenaka, S., Yamanaka, I., Tanabe, E., Genseki, A., & Otsuka, K. (2006). Formation of highly concentrated hydrogen through methane decomposition over Pd-based alloy catalysts. *J. Catal., 238*, 353-360
7. Ashok, J., Reddy , P. S., Raju , G., Subrahmanyam , M., & Venugopal , A. (2009). Catalytic Decomposition of Methane to Hydrogen and Carbon Nanofibers over Ni−Cu−SiO2 Catalysts. *Energ. Fuel., 23*(1), 5-13.
8. Lázaro, M. J., Echegoyen, Y., Suelves, I., Palacios, J. M., & Moliner, R. (2007). Decomposition of methane over Ni-SiO2 and Ni-Cu-SiO2 catalysts: Effect of catalyst preparation method. *Appl. Catal. A Gen., 329*(1), 22-29.
9. Ashour, S. S. (2014). Structural, textural and catalytic properties of pure and Li-doped NiO/Al2O3 and CuO/Al2O3 catalysts. *J. Saudi Chem. Soc., 18*(1), 69-76.
10. Gregg, S., & Sing, K. (1982). Adsorption, surfacearea and porosity. London: Academic Press Inc.
11. Orellana, F., Lisperguer, J., & Nuñez, C. (2014). Synthesis and characterization of polypropylene-silica, alumina and titania nanoparticles, prepared by melting. *J. Chil. Chem. Soc., 59*(1), 2389-2393.
12. De Llobet , S., Purón , H., Pinilla , J., Moliner , R., Millán , M., & Suelves , I. (2013). Tailored synthesis of organised mesoporous aluminas prepared by non-ionic surfactant templating using a Box-Wilson CCF design. *Micropor. Mesopor. Mat., 179*, 69-77
13. Yalamaç, E., Trapanib, A., & Akkurt, S. (2014). Sintering and microstructural investigation of gamma alpha alumina powders. *J. Chil. Chem. Soc, 17*, 2-7.
14. Jiménez , V. (2011). Síntesis, activación química y aplicaciones de nanoestructuras de carbono. *tesis para optar el grado de Doctor en Ingeniería Química*(Universidad de Castilla – La Mancha).
15. De Llobet, S., Pinilla, J. L., Moliner, R., & Suelves, I. (2015). Effect of the synthesis conditions of Ni/Al2O3catalysts on the biogasdecomposition to produce H2-rich gas and carbon nanofibers. *Appl. Catal. B Environ, 165*, 457–465.

16. Lee, J.-H., Lee, E.-G., Joo, O.-S., & Jung, K.-D. (2004). Stabilization of Ni/Al2O3 catalyst by Cu addition for CO2 reforming of methane. *Appl. Catal. A Gen., 269*, 1-6.
17. Chen, J., Li, Y., Ma, Y., Qin, Y., & Chang, L. (2001). Formation of bamboo-shaped carbon filaments and dependence of their morphology on catalyst composition and reaction conditions. *Carbon, 39*, 1467-1475.